Título artículo / Títol article:	Fresnel phase retrieval method using an annular lens array on an SLM
Autores / Autors:	Vincent Loriot, Omel Mendoza Yero, Jorge Pérez Vizcaíno, Gladys Mínguez Vega, Jesús Lancis Sáez, Rebeca De Nalda, Luis Bañares
Revista:	Applied Physics B-Lasers and Optics v. 117, n. 1 (2014
Versión / Versió:	Preprint de l'editor
Cita bibliográfica / Cita bibliogràfica (ISO 690):	LORIOT, V.; MENDOZA YERO, O.; PÉREZ VIZCAÍNO, J., MÍNGUEZ VEGA, G.; LANCIS SÁEZ, J.; DE NALDA, R.; BAÑARES, L. Fresnel phase retrieval method using an annular lens array on an SLM. Applied Physics B-Lasers and Optics v. 117, n. 1 (2014), pp. 67-73
url Repositori UJI:	http://repositori.uji.es/xmlui/handle/10234/125205

Active wavefront compensation of broadband femtosecond laser pulses through pupil segmentation

Vincent Loriot,[1,2*] Omel Mendoza-Yero,[3] Jorge Pérez Vizcaino, [3] Gladys Mínguez-Vega,[3] Jesús Lancis Sáez,[3] Rebeca de Nalda,[1] and Luis Bañares.[2]

[1] *Instituto de Química Física Rocasolano, Consejo Superior de Investigaciones Científicas, 28006 Madrid, Spain.*

[2] *Facultad de Ciencias Químicas, Universidad Complutense de Madrid, 28040 Madrid, Spain*

[3] *GROC·UJI, Institut de Noves Tecnologies de la Imatge (INIT), Universitat Jaume I, 12080 Castelló, Spain.*

Abstract

Wavefront aberrations play a major role when focusing an ultrashort laser pulse to a high quality focal spot. Here, we report a novel method to measure and correct wavefront aberrations of a 30 femtosecond pulsed laser beam. The equipment is simple, as the method only requires a programmable liquid crystal spatial light modulator and a CCD camera. Wavefront retrieval is based on pupil segmentation, which allows us to determine the local phase that minimizes focusing errors due to wavefront aberration. Our method provide accurate results even when implemented with a low dynamic range cameras and polychromatic beams. Finally, the retrieved phase is added to a diffractive lens codified onto the spatial light modulator to experimentally demonstrate nearly diffraction-limited femtosecond beam focusing without refractive components.

Keywords: Diffractive optics, Ultrafast optics, Adaptive Optics, Spatial Light Modulation.

1. Introduction

Focusing ultrashort laser pulses to a small focal region is the key of a myriad of nonlinear optical phenomena such as microscopic imaging, manipulation and machining. However, wavefront aberrations originated by imperfections, misalignments and stress of the opticals mounts in the chains inside femtosecond amplifier systems enlarge the spatial dimensions of the focal spot. It is now well established that the measurement and the correction of wavefront aberrations of the laser pulse is crucial for high-quality stable focusing [1-3]. An adaptive optics system, which consists of a wavefront sensing device and a compensating unit, measures and corrects the wavefront aberrations of a laser pulse, and eventually delivers a nearly diffraction-limited focal spot to a target. The above device has been successfully applied in such different fields as to generate high laser intensities in the range of 10^{22} W/cm^2 [4,5], to increase the repetition rate of high-energy lasers [6] and to write optical waveguides in dielectric samples [7].

Accurate knowledge of the laser beam wavefront is the first step towards producing highly focused homogeneous intensity spots. Several phase-measurement methods have already been proposed and demonstrated. The most popular is the Shack-Hartmann wavefront sensor (SHWS) where the measurement of the local phase slopes of the wavefront provides the entire beam phase [1-7]. This technique requires a microlens array that divides the pulsed beam into a number of beamlets and has been implemented, for instance, to test the temporal stability of pulsed laser beams [8]. Achromatic lateral-shearing interferometers are particularly suited for the measurement of the wavefront of broadband ultrashort laser pulses because of its achromaticity [9].

Also, the angular and spectral dependences of the second-harmonic generation conversion efficiency in uniaxial crystals have been used for phase measurement [10]. On the other hand, the Fresnel phase-retrieval method offers a relatively simple configuration as the phase of the pulsed beam is reconstructed from only two intensity distributions at two planes along the optical axis that are measured by means of simple CCD cameras. This technique has been successfully employed for terawatt-class femtosecond laser pulses with accuracy better than $\lambda/30$ peak to valley [11,12]. The iterative Fourier transform algorithm is used to achieve an acceptable solution for the wavefront and the effects of the dynamic range of the sensor, the intensity noise, and the wavelength-dependent error in wavefront reconstruction are considered. Concerning wavelength error, the value was demonstrated to be negligible for long pulses of 100 fs but also claimed that increases proportionally with the bandwidth for shorter pulses.

On a completely different context, liquid-crystal displays working as electronically addressed spatial light modulators (SLM) have been widely used to generate programmable diffractive lenses (DL) to focus continuous wave laser radiation, even monochromatic [13] or polychromatic [14]. Also, array of lenses have been codified to implement a programmable SHWS [15]. Now, the mathematical models to optimize encoding of the lens function in a device constrained by the pixelated structure and the phase quantization of the SLM are well understood [16]. Although, such lenses suffer from a relatively low pupil diameter and high focal length they allow for an electronically controlled variable focal length. But, what is more important, the use of this kind of modulators introduces the benefit of local beam control of the phase of the lens which allows for minimizing focusing errors due to wavefront aberrations.

Here, we present a novel technique for wavefront retrieval of short pulses coming from commercial amplifier systems running at mJ energy levels and temporal pulse durations at tenths of fs. The method requires the implementation of a DL onto the SLM, which is subsequently apertured through a set of concentric rings in a sequential way. Also, the intensity is measured with a CCD camera at the focal plane for each ring-shaped zone. As a result, our technique is particularly well-fitted for the measurement of the drop in diffraction efficiency at the outermost radial zones of the DL due to the reduced number of phase steps available for codifying the lens function. Our method permits to deal properly with the different arrival time of pulses coming from different radial locations at the SLM plane. The segmentation of the pupil plane into subregions to measure wavefront aberrations was recently introduced in the field of high-resolution imaging in biological tissue [17]. In a second step, the lens function was codified onto the SLM, with the local phase modified in accordance with the results achieved at the sensing stage, and a laboratory experiment concerning to the diffractive focusing of a 30 fs laser beam was carried out. Yet, our technique also opens the possibility of real-time fine-tuning of laser beams through the programmable nature of phase-only SLMs.

2. Optical setup

We present a schematic of our experimental setup in Figure 1. An ultrashort laser source (FEMTOPOWER compact PRO from Femtolaser) emitted 30 fs light pulses at the central wavelength of 800 nm and repetition rate of 1 kHz. The pulsed beam was sent to a 4× all-mirror beam expander (BE) to better fit the active area of the SLM with an almost constant intensity beam and a pellicle beam splitter (BS) were inserted in the beam path. The transmitted beam was used to monitor the average power of the beam by means of a power meter (PM). The power was controlled using a variable attenuator consisting of a half-wave plate and a Glan-Thompson polarizer (not in the picture). The

reflected beam impinged onto a liquid-crystal phase-only SLM (PLUTO-NIR from Holoeye) having a spatial resolution of 1920 x 1080 pixels and pixel pitch of 8 microns.

To focus the beam, we encoded onto the SLM a quadratic phase factor corresponding to a DL. Initially, we sent to the modulator the gray levels corresponding to the quadratic phase $\phi(r)$ imparted by a lens of focal length f ; i.e, $\phi(r) = kr^2 / 2f$, with k the wave number and r the radial coordinate onto the SLM pupil. In practice the SLM displays the phase wrapped in 2π steps. Focusing artifacts (such as multiple focal lengths and higher-order diffractions) due to the pixilated and the quantized nature of the SLM were taken into account. Quantization effects originate aliasing at the outer regions of the lens since the available number of pixels to codify each wrapped zone decreases with the distance to the center due to the squared dependence of the phase with the radial coordinate. In practical terms, this effect fixes the ultimate limit for the available minimum focal length, which is given by $f = kD\Delta r / 2\pi$, with D the lens diameter and Δr the outermost zone width that must be longer than the pixel pitch. To overcome this limit, we encoded in the SLM a DL of 130 mm of focal length for 800 nm. The CCD camera (Ueye UI-1540M) was located at the focal plane.

Deviations from its ideal form were found and attributed to unanticipated spatial phase inhomogeneities over the pulsed laser beam that can be described completely by the wave aberration. It is defined as the difference between the perfect (plane) and the actual wavefront for every point at the pupil of the SLM for the mean wavelength. A perfect pulsed laser beam focuses to a circularly symmetric pattern. However, spatial phase inhomegeneities generate aberrations that produce a larger and, in general, asymmetric focal distribution. Wavefront aberrations were subsequently measured and corrected to achieve enhanced resolution and to generate high intensity in lenless pulsed beam focusing.

2.1. Wavefront sensing

To retrieve spatial phase inhomogeneities of the pulsed laser beam coming from the femtosecond system, the beam at the SLM plane was divided into N discrete zones that tile its whole active area and, thereby, was segmented into N beamlets individually controllable. Each zone corresponds to a circular ring whose inner, r_{in}, and outer radius, r_{out}, were chosen in such a way that the propagation time difference (PTD) for pulses originated at the two edges of the zone to the geometrical focus is smaller than the femtosecond pulse width. This propagation time difference can be calculated by the formula $(r_{out}^2 - r_{in}^2) / 2fc$, being c the speed of the light [18]. In our experiment we considered a PTD of 22 fs, i.e. the area of each ring was 5.32 mm^2. In addition we chose an approach based on ring overlapping. This means that one zone overlapped with the following by a distance equivalent to half of the PTD. With the above parameters our total number of ring was of N=23. As the pulse width reduces, more zones are needed to achieve an accurate approximation. The above effect is attributed to the increasing bandwidth of the pulse that introduces higher chromatic artifacts in the phase retrieval algorithm.

We then applied the quadratic phase pattern corresponding to a DL with focal length 130 mm only to one of the zones. The remaining zones were driven with a phase pattern corresponding to a diverging lens that causes the associated beamlets generate negligible effect at the focus, rendering them effectively ‘off’. We acquired an image at the focal plane using the sole remaining ‘on’ beamlet. An example of the SLM phase distribution corresponding to several ring-shaped zones used in the experiment can be found in Fig. 2 (a-c). To reduce the noise due to experimental fluctuations of the beam, we captured several images of the focal plane and averaged them. The focal irradiance

measured with the CCD for the previous ring positions are in Fig. 2 (d-f). Contribution of the innermost zone of the DL corresponds nearby to the Airy pattern as can bee seen in Fig. 2(d). However, as expected, the output pattern recorded by the CCD differs more from the ideal theoretical focal distribution of the homogeneous annulus for the outermost zones of the lens. This effect was attributed to the optical aberrations that have a strong dependence with the radial coordinate and prevents us to get a nice Airy spot when the whole area of the SLM is used to focus the beam. In Fig. 2 (g-i) we show results for the focal irradiance distribution generated by the above zones after wavefront sensing and compensation as is discussed throughout the rest of the paper. The key point is pupil segmentation that takes into account the broadband nature of short pulses and allows focusing nearly free of chromatic artifacts. As mentioned earlier, the longer the spectrum of the laser the higher the number of ring-shaped zones. The ideal number of ring corresponds to the one that allow us to recover the nearby Airy patter for each ring.

To retrieve the azimuthal modulation over the active ring, the angular variation was sampled at a number of reference points uniformly distributed at the SLM plane for subsequent linear interpolation. In our work we found that, for all the practical aberrations, 12 points are sufficient to recover the main information of the wavefront. As we deal with complex patterns 24 independent parameters are required (12 for the amplitude and 12 for the phase). To ensure that the fitting procedure is self-consistent, we also added the ring position and the width as free test parameters. The adjustment of the 26 parameters was obtained from a 2D least square fitting procedure where the values were determined to generate a focal distribution with the minimum Euclidean distance to the experimental irradiance distribution. This ring position and the width test parameters were checked in each reconstruction and were in agreement with the segmentation used in the experiment. With the remaining 24 parameters and by means of a linear interpolation we were able to obtain the retrieved intensity and phase as is shown in Fig. 3. In Fig 3 (b) we illustrated the reconstructed output intensity from the retrieved amplitude and phase. The agreement between the measurement and the 2D fit is satisfactory.

Next we repeated the previous procedure for the whole set of ring-shaped zones. To optimize the time required for the calculus, the final parameters obtained in one ring were used as the initials parameters for the next ring-shaped zone. The full phase over the SLM plane is generated through stacking the information obtained for each zone. The retrieved phase over the SLM pupil in our case is shown in Fig. 4 a), where we have omitted the constant and the linear phase terms as they don't provide relevant information. We can see that numeric noise is more intense for the innermost zone. This is due to the fixed number of reference points used to sample the zones of the SLM plane, which are closer for this zone.

To compare our results, we also calculated the aberrated wavefront with the Fresnel phase-retrieval method using the conventional iterative Fourier tranform algorithm (IFTA) [11,12]. We considered that the intensity over the SLM was constant and measured the focal pattern irradiance generated by the whole DL. In the iterative calculation, we analyzed the convergence of the algorithm by measuring the root mean square (rms) error between the image in the focal plane measured with the CCD and the reconstructed image. Because the rms error of the intensity approaches an asymptotic value after iteration of the order of 100–300, the number of iterations was fixed at 300. The retrieved phase is shown in Fig 4 (a). We can observe that for the border area of the pupil we have less information of the phase than the one obtained with the proposed pupil segmentation method.

2.2. Pulsed beam focusing

To provide a demonstration of the capabilities of our method, we designed an experiment for lensless focusing of a femtosecond pulsed beam. To this end we simple used a SLM and no additional optics. In the SLM we encoded the quadratic phase factor corresponding to a DL, together with the phase that corresponds to the wavefront correction for our laser beam. Let us mention here that the main drawback of the procedure (shared with other methods of diffractive correction of wavefront aberrations) is that the finite number of pixels of the SLM causes the efficiency of the encoded DLs to depend on the radial coordinate. This unwanted effect decreases the peak intensity of the pulses coming from the outer zones of the encoded DL. Satisfactorily, our method is well suited to measure the radial dependence as the active area of the SLM is sampled through ring-shaped zones. For each ring-shaped zone, we evaluated the mean power that arrives to the focal plane and the values were normalized at its maximum value. In Fig. 5 we show the dependence of the efficiency of our DL of 130 mm focal length with the ring number. Error bars correspond to the standard deviation, as several images per ring where used to calculate the corresponding efficiency. As expected from a theoretical point of view, focalization efficiency of the outermost ring is about 40% as the DL is encoded with only two levels of phase [19].

Although compensation of the reduction in the radial drop of the diffraction efficiency is out of the scope of this paper, let us mention two different procedures to partially mitigate this effect. On the one hand, codification of DLs with a longer focal length as the outermost zone width is higher. Unfortunately there are some applications where this is not an option. On the othe hand, to guarantee a constant radial response it is possible to reduce the efficiency of the inner parts of the lens by controlling the designing parameters thorugh the maximum value of the wrapped phase [20]. In this way, the efficiency of lens can be made constant over the whole radius but at the price of generating more than one focus and consequently reducing the global energy derived to the main focal plane.

Finally let us compare in Fig. 6 the irradiance distribution in the focal plane of the encoded SLM in three different cases: a) without wavefront correction, b) with the wavefront correction provided by the Fresnel phase-retrieval method and c) with our pupil segmentation method. It appears clear that the spatial phase has a strong influence on the focalization of the pulse. In Fig. 7(a), the peak intensity is quite low due to the fact that aberrations causes a blurring of the image. With the Frenel phase-retrieval method, most of the problems has been corrected but the spatial compression is still not perfect. We attribute this fact to the poor quality of the image in Fig 6a) used to retrieved the phase. The quantizing level of the CCD camera and the broad spectrum of the laser pulse cause the blurring of the image, which results in a loss of resolution for the iterative method. However, pupil segmentation provides a stronger pulse focalization and, furthermore, the circular symmetry of the output pattern is recovered demonstrating that the SLM provides a convenient way to steer all rays to the focal point. So segmentation of the pupil plane into subregions to measure wavefront aberrations seems to be a powerful and simple technique when high accuracy is required even with polychromatic pulsed beams.

3. Conclusions

In this paper, we present an innovative spatial phase retrieval method based on pupil segmentation. To implement our method only an SLM and a CCD camera are needed. The pupil

plane correspond to the SLM, where a DL is encoded, and the output plane is the focal plane where the CCD is placed. The pupil plane is decomposed into overlapped concentric rings and, at the same time, the corresponding irradiance for each ring is recorded with the CCD. By means of a least square fitting the phase and amplitude distribution of the input beam over the SLM plane was retrieved. In our experiment the amplitude was flat and the phase was compared with the one obtained with the Fresnel phase retrieval method. We found that our proposal provides more accurate results. To test our method we did an experiment based on lensless focusing a 30 fs femtosecond laser beam. To increase the quality of the focal spot aberrations were corrected. The complex conjugate phase of the retrieved phase was encoded onto the SLM together with the DL. We observed that the spatial quality and energy of the focal spot obtained at the focal plane are higher when compared with conventional Fresnel phase retrieval method. This was attributed to pupil segmentation that allow to overcome the limitations associated with the poor dynamical range of conventional CCD cameras. This advantage is even crucial with multi-chromatic coherent beam such as the 30-fs pulse employed in the present experiment. In this case, we demonstrated that pupil segmentation is a powerful technique to overcome the additional blurring associated to chromatic aberrations in Fresnel phase-retrieval method. The adaptation of the Fresnel phase-retrieval method to the pupil segmentation technique will be seen elsewhere.

Acknowledgements

This work was supported by the Spanish Ministerio de Economia y Competitividad (MINECO) and FEDER through the projects FIS2010-15746, SAUUL (CSD2007-00013) and CTQ2008-02578. Also, financial support from the Generalitat Valenciana through project PROMETEO/2012/021 Fundació Caixa-Castelló through project P11B2010-26 and European network ITN FASTQUAST (PITN-GA-2008-214962) is acknowledged. The authors are grateful to the Serveis Centrals d'Intrumentació Científica of the Universitat Jaume I for the use of the femtosecond laser.

References

1. K. Akaoka, S. Harayama, K. Tei, Y. Maruyama, and T. Arisawa, Proc. SPIE **3265**, 219 (1998).
2. B. Schäfer, K. Mann, G. Marowsky, C. P. Hauri, J. Biegert, and U. Keller, Proc. SPIE **5918**, 59180P
3. T. A. Planchon, J. –P. Rousseau, F. Burgy, G. Chériaux, and J.-P. Chambaret, Opt. Commun. **252**, 222 (2005).
4. S.-W. Bahk, P. Rousseau, T. A. Planchon, V. Chvykov, G. Kalintchenko, A. Maksimchuk, G. A. Mourou, and V. Yanovsky, Opt. Lett. **29**, 2837 (2004).
5. V. Yanovsky, V. Chvykov, G. Kalinchenko, P. Rousseau, T. Planchon, T. Matsuoka, A. Maksimchuk, J. Nees, G. Cheriaux, G. Mourou, and K. Krushelnick, Opt. Express **16**, 2109 (2008).
6. B. Wattellier, J. Fuchs, J. P. Zou, K. Abdeli, C. Haefner, and H. Pépin, Rev. Sci. Inst. **75**, 5186 (2004).
7. A. Ruiz de la Cruz, A. Ferrer, W. Gaweld, D. Puerto, M. Galván Sosa, J. Siegel, and J. Solis, Opt. Express **17**, 20853 (2009).
8. J. M. Bueno, B. Vohnsen, L. Roso, and P. Artal, Appl. Opt. **49**, 770 (2009).
9. J.-C. Chanteloup, F. Druon, M. Nantel, A. Maksimchuk, and G. Mourou, Opt. Lett. **23**, 621 (1998).
10. R. Borrego-Varillas, C. Romero, J. R. Vázquez de Aldana, J. M. Bueno, and L. Roso, Opt. Express **19**, 22851 (2011).
11. S. Matsuoka and K. Yamakawa, J. Opt. Soc. Am. B **17**, 663 (2000).
12. T. M. Jeong, C. M. Kim, D.-K. Ko, and J. Leet, J. Opt. Soc. Kor. **12**, 186 (2008).
13. J. L. Martínez, I. Moreno, and E. Ahouzi, Eur. J. Phys. **27**, 1221 (2006).
14. A. Márquez, C. Iemmi, J. Campos, and M. J. Yzuel, Opt. Lett. **31**, 392 (2006).

15. J. Arines, V. Durán, Z. Jaroszewicz, J. Ares, E. Tajahuerce, P. Prado, J. Lancis, S. Bará, and V. Climent,, Opt. Express **15**, 15287 (2007).
16. E. Carcolé, J. Campos, and S. Bosch, Appl. Opt. **33**, 162 (1994).
17. N. Ji, D. E. Milkie, and E. Betzig, Nature Methods **7**, 141 (2010).
18. G. Mínguez-Vega, O. Mendoza-Yero, J. Lancis, R. Gisbert, and P. Andrés, Opt. Express. **16**, 16993 (2008).
19. S. Sinzinger and J. Jahns, "Microoptics," (Wiley VCH, Weinheim, Germany, 2003).
20. V. Moreno, J. F. Román, and J. R. Salgueiro, Am. J. Phys. **65**, 556 (1997).

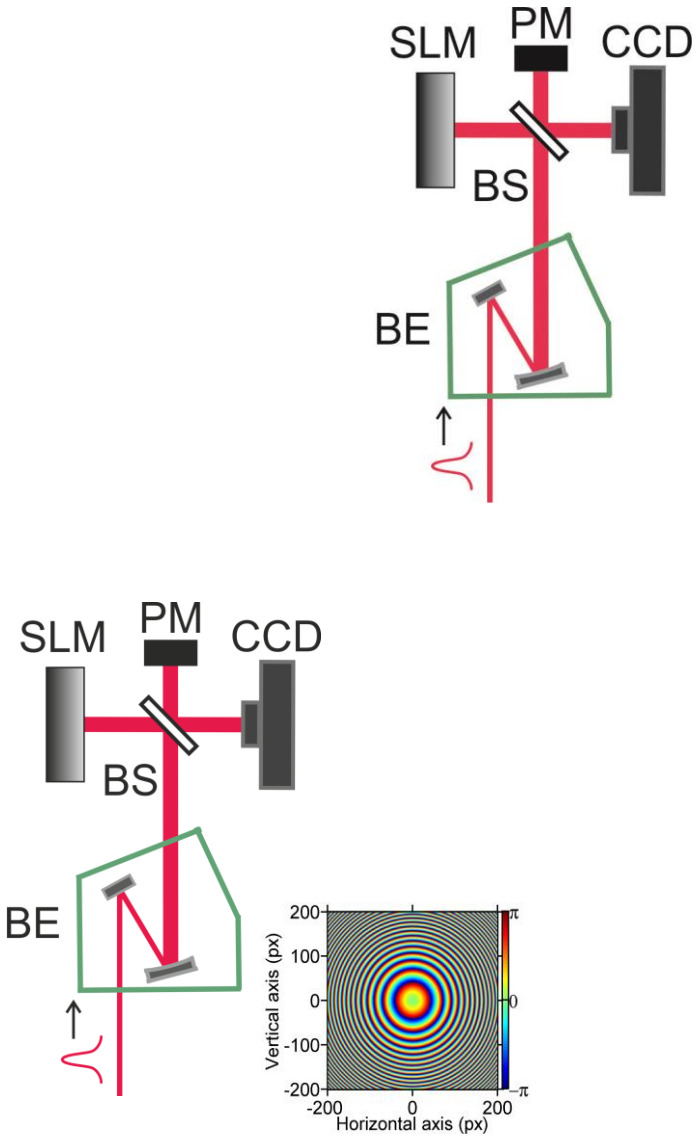

Figure 1. Schematic of the optical setup. In the inset, phase transmission function encoded in the central 400 × 400 pixels of the SLM corresponding to a DL.

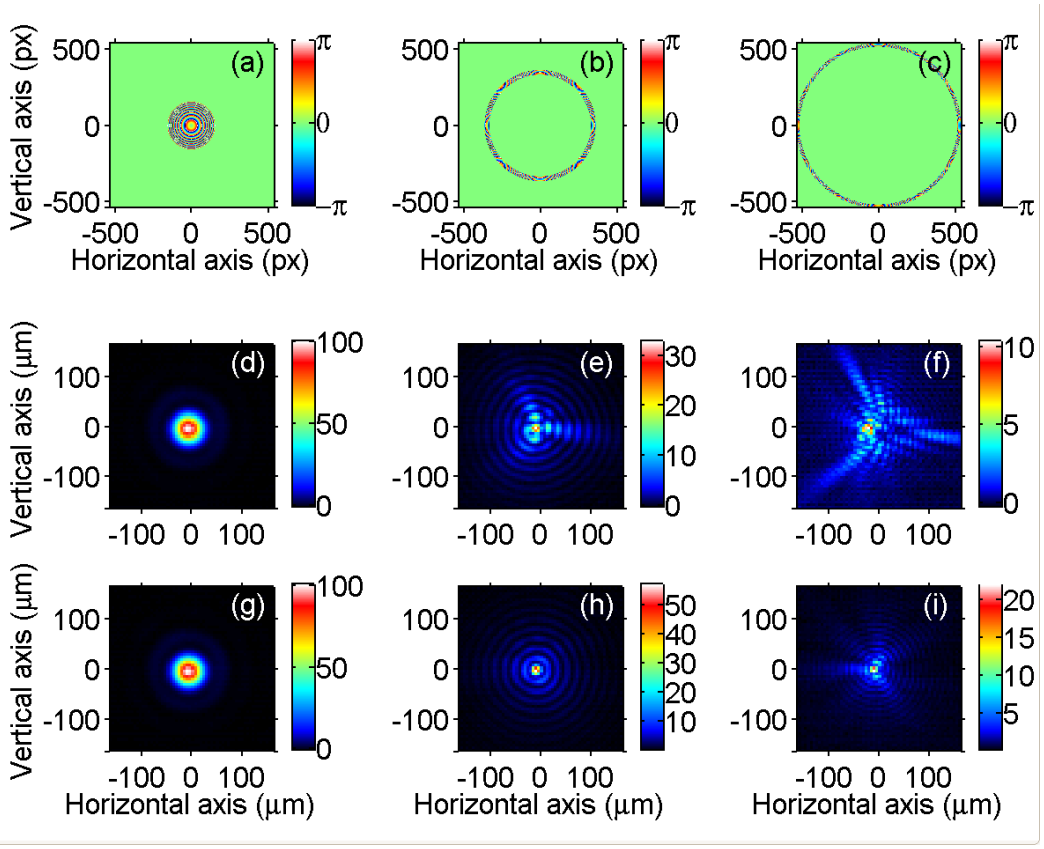

Figure 2. (a-c) Phase transmission function encoded in the SLM corresponding to a DL with a ring shape. The measured irradiance in the focal plane for each ring without (d-f) and with (g-i) wavefront correction. PONER EL NÚMERO DE ANILLO son 1, 10 y 23.

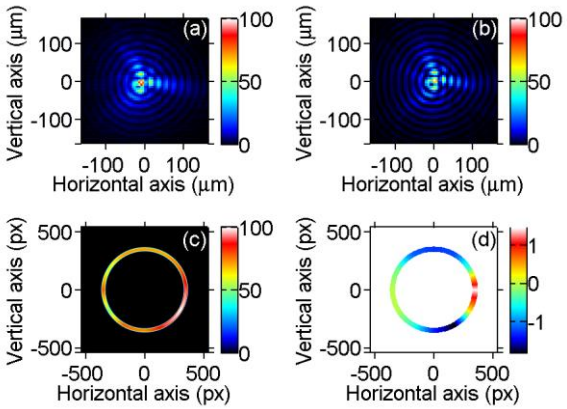

Figure 3. Phase recovery procedure for a ring-shaped zone over the SLM plane: a) Experimental measurement of the focal irradiance; b) Calculated irradiance distribution from the fitted phase; c) retrieved intensity which for our experiment is almost uniform; d) retrieved phase. LA PALETA DE COLOR SE PUEDE PONER EN NIVELES DE GRIS EN c) el anillo es el 10

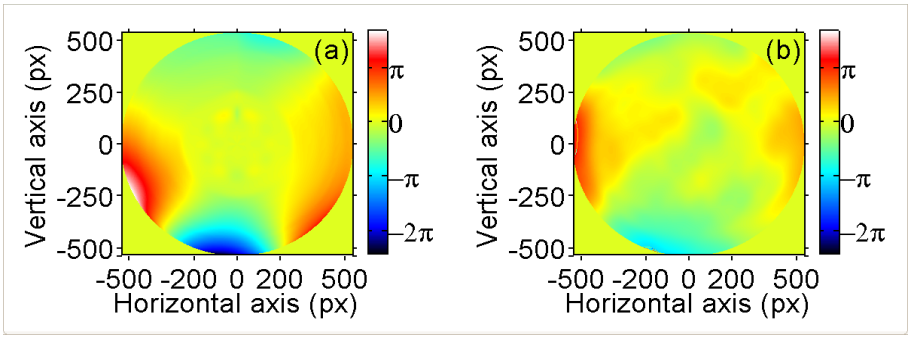

Figure 4: Spatial phase reconstruction perform with (a) the pupil segmentation method (b) Fresnel phase retrieval method.

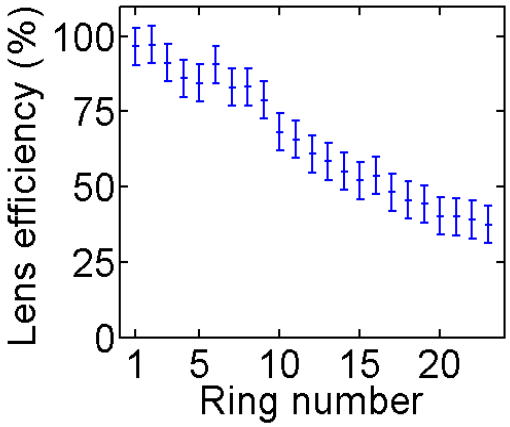

Figure 5: Diffraction efficiency of each of the rings used to segment the DL.

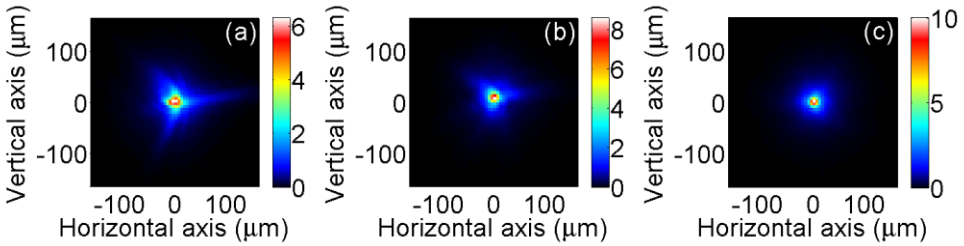

Figure 6: Measurement of the full beam (a) Without any correction of the spatial phase, (b) using Fresnel phase retrieval correction and (c) with the correction of the spatial phase presented in the article